Hindawi Publishing Corporation
Research Letters in Physics
Volume 2008, Article ID 891324, 5 pages
doi:10.1155/2008/891324

Research Letter

Experimental Investigation of the Transition to Spatiotemporal Chaos with a System-Size Control Parameter

Daniel R. Spiegel and Elliot R. Johnson

Department of Physics and Astronomy, Trinity University, San Antonio, TX 78212, USA

Correspondence should be addressed to Daniel R. Spiegel, dspiegel@trinity.edu

Received 2 January 2008; Accepted 2 April 2008

Recommended by Celso Grebogi

Using a localized laser-heating method to allow the use of system size as a control parameter, we experimentally investigate, using liquid-crystal electroconvection with soft boundary conditions, the onset of spatial temporal chaos (STC) with increasing system size. We find that temporal periodicity is significantly quenched as the system size increases. The increase of the fourth moment (kurtosis) of the temporal Fourier transform provides a very useful quantitative measure of the loss of temporal periodicity (hence the onset of STC) as the pattern size increases, and also provides a simple means for determining a natural chaotic length scale. This length scale is comparable to the length of vertical rows observed in the original pattern. Our experiments, thus, imply that there are well-defined building blocks, which in our case are easily visualized, that control the dynamics in STC liquid crystal convection. The results of our experiments appear to be consistent with the conclusions of recent STC computer simulations carried out by Fishman and Egolf.

1. INTRODUCTION

The understanding of chaotic dynamics in a spatially extended system with many degrees of freedom that is driven far from equilibrium, referred to as spatiotemporal chaos (STC), is still far from complete. Indeed, a rigorous predictive statistical STC model does not exist [1], in spite of the large amount of recent attention dedicated to STC including a number of important computer simulations. Fishman and Egolf [1] have found that deviations from extensivity, revealed in high-resolution simulations of the one-dimensional complex Ginzburg-Landau (CGL) equation, did indeed occur for small system sizes, and concluded that CGL STC must be composed of definitive weakly interacting building blocks, each containing about two degrees of freedom. Certainly, one may then hope to formulate a nonequilibrium statistical mechanical model of STC based on the building block interactions [2]. According to Fishman and Egolf, microextensive behavior [3, 4] is observed in large systems because building blocks separated by a large distance should be essentially uncorrelated.

Although the use of the system size as a control parameter has been a powerful tool in STC computer simulations, it is very difficult to vary this parameter *experimentally* [5–16] in a well-controlled manner, and the usual experimental hard boundary conditions (either Neumann or Dirichlet) can significantly placate the chaotic behavior one is attempting to study in smaller STC systems [17]. In the case of planar electroconvection in nematic liquid crystals, however, we have shown recently [18, 19] that modest laser heating can be used to produce spatially localized patterns, since the electroconvection threshold voltage decreases with increasing temperature [19]. By varying the size of the laser-cross-section incident on the sample, we therefore have a systematic manner of controlling the size of a convection pattern without introducing hard boundary conditions.

In planar eletroconvection, the voltage control parameter is defined as $\epsilon = (V/V_0)^2 - 1$, where V_0 is the threshold electroconvection voltage at the applied AC frequency. In our experiments, the laser-generated temperature profile results in a threshold voltage that depends on position. The first rolls appear where the temperature is largest, at a threshold

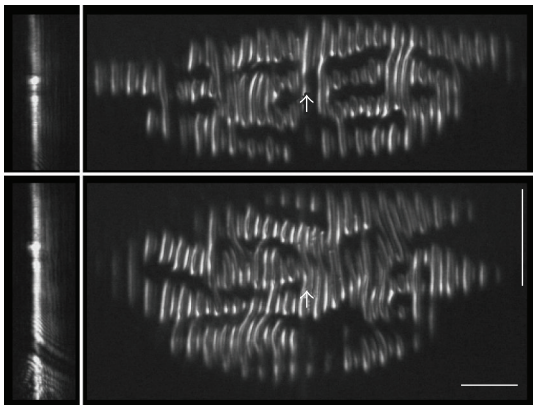

Figure 1: Two different laser cross-sections, shown on the left, are used to generate two spatiotemporal chaotic (STC) patterns of different sizes. x and y are horizontal (along the director) and vertical, respectively. Each pattern is driven at a fixed voltage-control parameter of $\epsilon_{\max} = 0.75$. The horizontal white bar in the lower-right corner represents a length of 100 μm, and the vertical white bar on the right, which we will argue, represents the natural chaotic length scale for our experiments, and corresponds to a length of 171 μm. The laser light transmitted through the sample is blocked from the detector using an optical filter; the actual positions of the laser cross-sections within the STC patterns are indicated by the white arrows.

voltage of $V_{0,\min}$. The voltage-control parameter, therefore, takes its maximum value $\epsilon_{\max} = (V/V_{0,\min})^2 - 1$ at this position. We set $\epsilon_{\max} = 0.75$ at an applied frequency of 377 Hz (which is well above the voltage required to generate STC [16, 20]) throughout this work by measuring $V_{0,\min}$ independently for each individual laser-controlled pattern investigated. Our approach is very different than previous STC electroconvection experiments [21–23].

Our basic experimental procedure can be understood with reference to Figure 1, in which x (the director axis) and y are taken in the horizontal and vertical directions, respectively. Following our usual procedure [18], we employ 40 μm-thick samples of MBBA doped at 0.2 wt% with a blue-absorbing dye (methyl red). On the left-hand side of the figure, we show two different 488 nm laser-beam cross-sections. The length in the y direction of the laser-line cross-section incident on the sample is set by cylindrical lenses and an adjustable knife-edge slit that is placed about 2 cm above the sample. The pattern aspect ratio is defined by the fact that the mean roll spacing is about 1/3 the sample thickness. The convection patterns generated using these cross-sections, each driven using a voltage-control parameter of $\epsilon_{\max} = 0.75$, are shown on the right-hand side of the figure. In Figure 1, the pattern size is larger in the y-direction for the laser-cross-section that is longer in the y-direction. In this manner, we may use the length of the laser cross-section as a system-size control parameter while holding $\epsilon_{\max}$ fixed. The laser cross-section is not spatially uniform due to knife-edge and single-slit diffraction; however, this nonuniformity is not reflected in convection patterns. We believe this is due to strong advection within the pattern creating a uniform temperature profile after the patterns forms, as we have argued previously [18].

Spacetime contour plots for pattern dynamics obtained at two different system sizes are shown in Figure 2. To construct the spacetime portraits, we study the variation of the pattern intensity over a long strip, parallel to the director (x-direction), located vertically near the center of the pattern. The length of the laser-beam cross-section employed, which controls the size of the pattern in the y direction, is noted at the top of each figure. Although both profiles show significant disorder, there is an important difference: the smaller-sample-size profile on the left displays some regions, where temporal periodicity is clearly evident (e.g., near $x = 600\,\mu$m on the left-hand spacetime portrait). To better understand this difference, we have in Figure 3 Fourier transformed the vertical time axis of Figure 2, showing the Fourier-frequency power spectra at different positions along the x-axis. The power-spectrum intensities have been multiplied by a factor of the Fourier frequency f so that $1/f$-noise would not dominate the spectra. In these "space-frequency" diagrams, it is clear that the smaller-system-size (left-hand) temporal Fourier spectra at different spatial positions is considerably more peaked in frequency than the larger-system-size spectra on the right.

In order to quantify the increasing spread in Fourier power spectra with increasing system size, one needs to calculate moments of the power spectra. We have found that the second moment (variance) does not couple to the outer wings of the power spectra; thus, we have instead calculated a fourth moment (a kurtosis-type function K): $K = \sum_i (P_i f_i)(f_i - \overline{f})^4 / \sum_i (P_i f_i)$, where the sum is over temporal frequencies f_i, and where P_i is the component of the Fourier power spectrum at temporal frequency f_i, spatially averaged over the x-direction, and $\overline{f} = \sum_i (P_i f_i) f_i / \sum_i P_i f_i$. Since K is highly sensitive to the portion of the Fourier power spectrum lying outside a main central peak, K provides a quantitative measure of the loss of temporal periodicity content within the pattern. To keep the analysis as simple as possible, we did not attempt to measure moments higher than fourth order. In Figure 4, we plot K as a function of the laser cross-section length, which controls the pattern size in the y-direction. Error bars are obtained by measuring K using space-frequency plots obtained from five different horizontal strips within the pattern. The kurtosis shows a clear systematic increase, by over an order of magnitude, with system size. The dashed line in Figure 4 shows the value for K obtained when an identical liquid crystal displaying STC over the entire sample (about 1 cm^2), with no laser excitation present, is also driven at a control parameter of $\epsilon = 0.75$. Our measurements at the largest laser-controlled pattern sizes approach this value, lending consistency to the idea that periodicity content is systematically quenched to a small final value as the system approaches an "infinite" size. It should be noted that the large-system-size measurement was treated in the same way as the laser-induced patterns: we study the variation of the pattern intensity over a long strip, parallel to the director (x-direction), which has the same width as the strips studied in the laser-induced patterns.

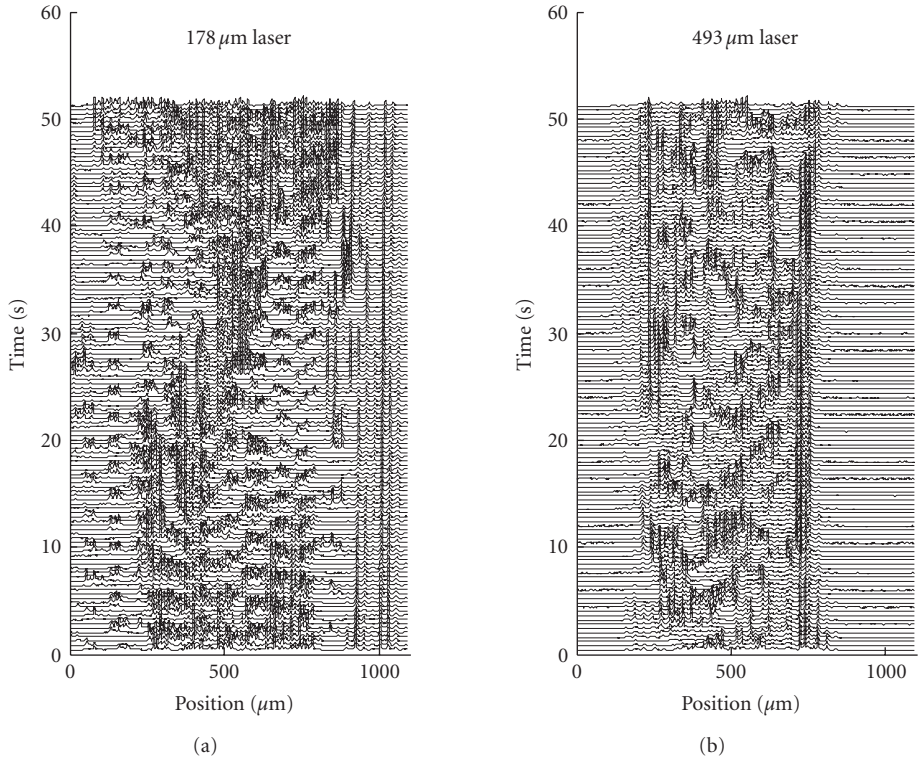

Figure 2: Spacetime contour diagram for patterns of different sizes, with the "laser" number at the top representing the length of the laser-beam cross-section, which sets the width of the pattern perpendicular to the director.

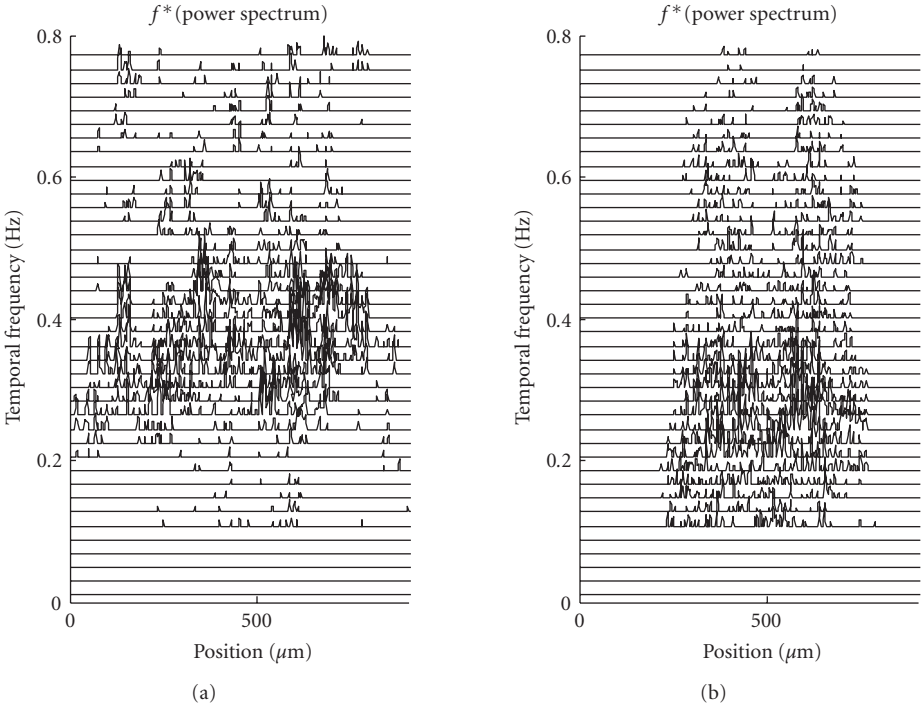

Figure 3: "Space-frequency diagrams": contour plots in which the time axis of Figure 2 has been Fourier transformed to obtain the power spectra, multiplied by the frequency f to reduce the effects of $1/f$ noise.

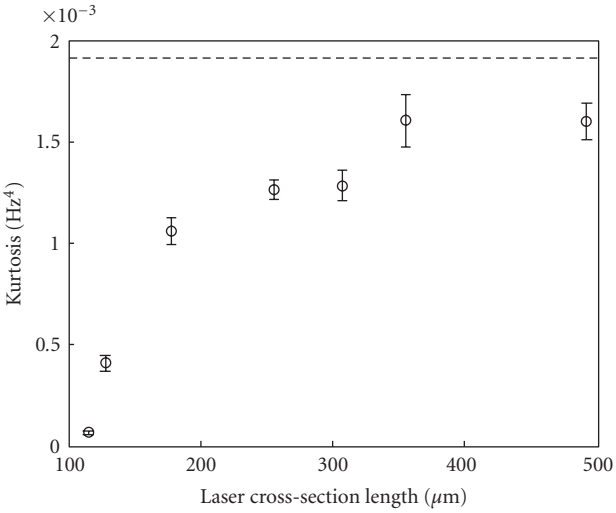

Figure 4: The fourth moment, the kurtosis K is plotted as a function of the laser-cross-section-size control parameter, which sets the system size. The dashed line shows the kurtosis obtained for a much larger 1-cm^2 region driven at the same voltage-control parameter in the absence of laser light.

The plot of the kurtosis for different pattern sizes can now be used in a simple way to provide a new experimental chaotic length scale l_c. A natural length scale in terms of a pattern size required for the quenching of the periodicity and the onset of complete nonperiodic STC is the pattern size at which the kurtosis obtains one half of its infinite-system-size value. From Figure 4, this length scale is $l_c = 171\,\mu$m. A vertical white bar corresponding to this length has been placed in Figure 1. It is apparent from this figure that l_c is the length of two or three attenuated rolls. We conclude from this that the STC is apparently controlled by the interaction between attenuated rolls, and that the attenuated rolls themselves are the fundamental building blocks of the STC that we observe. For pattern sizes (measured along y) that are comparable to l_c, two or three attenuated-roll building blocks will be highly correlated as coupled oscillators and can maintain temporally periodic dynamics. For large pattern sizes compared to l_c, distant rolls are completely decorrelated and temporal periodicity is lost, so that the pattern displays chaotic dynamics with a much wider frequency spectrum, as seen in the transition to chaos in classic single-particle systems such as the damped driven pendulum. Our experimental conclusions appear to be very consistent with the CGL computer simulations of Fishman and Egolf [1], who found that the increase in fractal dimension D was quantized as the size of a small system was increased from zero to include two or three building blocks, but that as the system size was further increased to contain many more building blocks, quantized increases in D could not be detected. Our main point is that in both our experiments and in the computer simulations of Fishman and Egolf [1], the STC is composed of well-defined building blocks, but one must work with pattern sizes that are only large enough to contain two or three building blocks in order to detect the presence of the building blocks and measure their sizes.

ACKNOWLEDGMENTS

We gratefully acknowledge very helpful conversations with Guenter Ahlers, Stephen Morris, Harry Swinney, and Richard Wiener. This work was supported by grants from the National Science Foundation and the Petroleum Research Fund, administered by the American Chemical Society.

REFERENCES

[1] M. P. Fishman and D. A. Egolf, "Revealing the building blocks of spatiotemporal chaos: deviations from extensivity," *Physical Review Letters*, vol. 96, no. 5, Article ID 054103, 4 pages, 2006.

[2] D. A. Egolf, "Equilibrium regained: from nonequilibrium chaos to statistical mechanics," *Science*, vol. 287, no. 5450, pp. 101–104, 2000.

[3] S. Tajima and H. S. Greenside, "Microextensive chaos of a spatially extended system," *Physical Review E*, vol. 66, no. 1, Article ID 017205, 4 pages, 2002.

[4] H. Xi, R. Toral, J. D. Gunton, and M. I. Tribelsky, "Extensive chaos in the Nikolaevskii model," *Physical Review E*, vol. 62, no. 1, pp. R17–R20, 2000.

[5] S.-Q. Zhou and G. Ahlers, "Spatiotemporal chaos in electroconvection of a homeotropically aligned nematic liquid crystal," *Physical Review E*, vol. 74, no. 4, Article ID 046212, 7 pages, 2006.

[6] S. W. Morris, E. Bodenschatz, D. S. Cannell, and G. Ahlers, "Spiral defect chaos in large aspect ratio Rayleigh-Bénard convection," *Physical Review Letters*, vol. 71, no. 13, pp. 2026–2029, 1993.

[7] Y. Hu, R. E. Ecke, and G. Ahlers, "Transition to spiral-defect chaos in low prandtl number convection," *Physical Review Letters*, vol. 74, no. 3, pp. 391–394, 1995.

[8] P. D. Mininni, D. O. Gómez, and G. B. Mindlin, "Biorthogonal decomposition techniques unveil the nature of the irregularities observed in the solar cycle," *Physical Review Letters*, vol. 89, no. 6, Article ID 061101, 4 pages, 2002.

[9] D. J. Patil, B. R. Hunt, E. Kalnay, J. A. Yorke, and E. Ott, "Local low dimensionality of atmospheric dynamics," *Physical Review Letters*, vol. 86, no. 26, pp. 5878–5881, 2001.

[10] A. Ghosh, V. Ravi Kumar, and B. D. Kulkarni, "Parameter estimation in spatially extended systems: the Karhunen-Loève and Galerkin multiple shooting approach," *Physical Review E*, vol. 64, no. 5, Article ID 056222, 8 pages, 2001.

[11] D. A. Egolf, I. V. Melnikov, and E. Bodenschatz, "Importance of local pattern properties in spiral defect chaos," *Physical Review Letters*, vol. 80, no. 15, pp. 3228–3231, 1998.

[12] A. Palacios, G. H. Gunaratne, M. Gorman, and K. A. Robbins, "Karhunen-Loève analysis of spatiotemporal flame patterns," *Physical Review E*, vol. 57, no. 5, pp. 5958–5971, 1998.

[13] Y. Zhang, M. Dai, Y. Hua, W. Ni, and G. Du, "Digital communication by active-passive-decomposition synchronization in hyperchaotic systems," *Physical Review E*, vol. 58, no. 3, pp. 3022–3027, 1998.

[14] M. Münkel, F. Kaiser, and O. Hess, "Stabilization of spatiotemporally chaotic semiconductor laser arrays by means of delayed optical feedback," *Physical Review E*, vol. 56, no. 4, pp. 3868–3875, 1997.

[15] Q. Ouyang and H. L. Swinney, "Transition to chemical turbulence," *Chaos*, vol. 1, no. 4, pp. 411–420, 1991.

[16] S. Kai and W. Zimmermann, "Pattern dynamics in the electrohydrodynamics of nematic liquid crystals," *Progress of Theoretical Physics Supplement*, no. 99, pp. 458–492, 1989.
[17] B. J. Gluckman, C. B. Arnold, and J. P. Gollub, "Statistical studies of chaotic wave patterns," *Physical Review E*, vol. 51, no. 2, pp. 1128–1147, 1995.
[18] N. C. Giebink, E. R. Johnson, S. R. Saucedo, et al., "Dynamics of laser-induced electroconvection pulses," *Physical Review E*, vol. 69, no. 6, Article ID 066303, 10 pages, 2004.
[19] D. R. Spiegel, E. R. Johnson, and S. R. Saucedo, "Amplitude modulation and relaxation-oscillation of counterpropagating rolls within a broken-symmetry laser-induced electroconvection strip," *Physical Review E*, vol. 73, no. 3, Article ID 036317, 8 pages, 2006.
[20] E. Plaut and W. Pesch, "Extended weakly nonlinear theory of planar nematic convection," *Physical Review E*, vol. 59, no. 2, pp. 1747–1769, 1999.
[21] N. Oikawa, Y. Hidaka, and S. Kai, "Defect chaos in a convective system limited by domain walls," *Journal of the Physical Society of Japan*, vol. 73, no. 11, pp. 2917–2920, 2004.
[22] T. Tóth-Katona and J. T. Gleeson, "Conductive and dielectric defects, and anisotropic and isotropic turbulence in liquid crystals: electric power fluctuation measurements," *Physical Review E*, vol. 69, no. 1, Article ID 016302, 10 pages, 2004.
[23] M. Dennin, G. Ahlers, and D. S. Cannell, "Chaotic localized states near the onset of electroconvection," *Physical Review Letters*, vol. 77, no. 12, pp. 2475–2478, 1996.